LUND UNIVERSITY

Direction-of-arrival estimation for closely coupled arrays with impedance matching

Lau, Buon Kiong; Bach Andersen, Jørgen

Direction-of-Arrival Estimation for Closely Coupled Arrays with Impedance Matching

Buon Kiong Lau, *Member, IEEE*

Department of Electrical and Information Technology
Box 118, Lund University
SE-221 00 Lund. Sweden
bkl@eit.lth.se

Jørgen Bach Andersen, *Life Fellow, IEEE*

Department of Electronic Systems
Aalborg University
9220 Aalborg. Denmark
jba@es.aau.dk

Abstract—**Conventionally, the spacing between adjacent elements in an antenna array are set at half-a-wavelength in order to obtain maximum spatial resolution while avoiding spurious sidelobes. However, for antenna arrays that are implemented in a compact manner, the spacing between the adjacent elements can be significantly less than half-a-wavelength. The small spacing between the antennas results in strong mutual coupling between the antennas, which has been shown to affect the performance of array algorithms, through modifying the antenna pattern and reducing the antenna efficiency. Recently, impedance matching techniques have been proposed for multiple antenna systems for diversity and MIMO applications, in order to counteract the aforesaid coupling effects. In this paper, we study the impact of different impedance matching conditions on the Cramer-Rao bound performance of direction-of-arrival estimation of closely coupled arrays. We demonstrate that an appropriate matching network can drastically improve the CRB performance with respect to both 50 ohm termination and the case of ideal antenna arrays with no coupling. For example, a ten-fold reduction in RMSE was obtained with the multiport conjugate match for a two signal scenario and an antenna separation of 0.1*wavelength.**

Keywords-Direction finding; mutual coupling, impedance matching; antenna arrays

I. INTRODUCTION

An antenna system with more than one antenna element can be utilized to greatly improve the performance of wireless communications, e.g. [1], [2]. This is particularly the case for multiple-input-multiple-output (MIMO) systems [3]-[5], which are being planned for upcoming communication systems such as IEEE 802.11n, IEEE 802.16e, and 3G long term evolution (LTE). In MIMO systems, multiple antenna elements are used at both the transmitter and the receiver. While there is usually less constraint on the separation distance between antennas at the base station, the implementation of multiple antenna systems on compact terminals, such as a mobile handset, is hampered by the problem of strong mutual coupling and high antenna correlation between closely spaced antennas [6].

Recently, multiport impedance matching networks have been shown to be an effective technique to mitigate the problems with coupling and correlation [7], [8], though at a cost of diminishing bandwidth [9]. However, the impact of such matching networks on the performance of other array techniques is still unknown. One such technique is direction-of-arrival (DOA) estimation, which can be an additional feature implemented on MIMO enabled compact handsets.

The effect of mutual coupling on DOA estimation has been studied in the context of fixed characteristic (or 50 ohm) termination [10]. The study reveals that in general coupling has no significant impact on the performance of DOA estimates. This is partly because the study pays no particular emphasis on very small antenna separations, even though it did point out that the influence of coupling increases with decreasing antenna separation [10].

In this paper, we focus on the performance of DOA estimation for compact antenna arrays, where the minimum separation between two adjacent antennas is less than half-a-wavelength. In particular, the impact of different impedance matching conditions on the Cramér-Rao lower bound (CRB) of DOA estimates is investigated.

The paper is organized as follows: Section II outlines the signal model used to investigate the effect of matching on closely coupled arrays. Based on this model, the CRB is presented in Section III. Section IV summarizes the four different impedance matching conditions considered in this study. Numerical examples are then presented in Section V. Finally, Section VI concludes the paper.

II. SIGNAL MODEL

With no loss in generality, we consider a uniform linear array (ULA) of N half-wavelength dipole antennas and inter-element spacing d. The ith component of the geometrical array factor (or steering vector) $\mathbf{a}(\Theta)$, where $i = 1, \ldots, N$, for a far-field narrowband signal of wavelength λ arriving from the direction $\Theta = (\theta, \phi)$ is given by [10]

$$\left[\mathbf{a}(\Theta)\right]_i = g(\theta)\exp\left[-j\,2\pi d \sin\theta \cos\phi\,(i-1)/\lambda\right], \quad (1)$$

where
$$g(\theta) = \lambda \cos\left(\frac{\pi\cos\theta}{2}\right)\bigg/(\pi\sin\theta) \quad (2)$$

is the dipole antenna pattern, azimuth angle $\phi = 0°$ corresponds to the +ve x-axis (or array endfire) and elevation $\theta = 0°$ the +ve z-axis. For simplicity, we limit our discussions in the following to signals incident on the azimuth plane, i.e. $\theta = 90°$. Thus, $\mathbf{a}(\Theta) = \mathbf{a}(\phi, 90°) = \mathbf{a}(\phi)$.
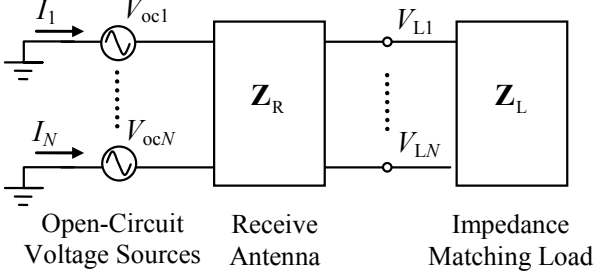
Fig. 1   Block diagram of receive subsystem.

Suppose the array receives M signals, where the mth signal $s_m(t)$ arriving from a distinct azimuth angle ϕ_m. The array output is given by the vector

$$\mathbf{x}(t) = \mathbf{A}\mathbf{s}(t) + \mathbf{n}(t), \tag{3}$$

where $\mathbf{A} = \left[\mathbf{a}(\phi_1), \ldots, \mathbf{a}(\phi_M) \right]$, $\mathbf{s}(t) = \left[s_1(t), \ldots, s_m(t) \right]^T$, $\mathbf{n}(t) = \left[n_1(t) \cdots n_N(t) \right]^T$, $n_i(t)$ is the noise output of the nth sensor. $\mathbf{n}(t)$ and $\mathbf{s}(t)$ are assumed to be stationary, zero mean, and uncorrelated with each other. Moreover, the noise at the different antennas are assumed to be circularly Gaussian distributed and have a common variance (or power) σ_n^2. The covariance matrix is given by

$$\mathbf{R_x} = \mathrm{E}\left[\mathbf{x}(t)\mathbf{x}^H(t) \right] = \mathbf{A}\mathbf{R_s}\mathbf{A}^H + \sigma_n^2 \mathbf{I}_N, \tag{4}$$

where the signal covariance matrix $\mathbf{R_s} = E\left[\mathbf{s}(t)\mathbf{s}^H(t) \right]$, and $\mathbf{I}_N$ is the $N \times N$ identity matrix.

Following the approach in [10] and [11], we apply the Z-parameter representation to include the effect of coupling and impedance matching into the array representation. We begin with the Z-parameter model of the receiver as in Fig. 1. When the antennas are open-circuited, the signals impinging on the antennas produce an open-circuit (or induced) voltage V_{oci} across the input port of the ith antenna. The voltages can then be represented as Thevenin-equivalent voltage sources. When the antennas are connected to an impedance matching load (the equivalence of matching network and load), it interacts with the antenna to produce the currents $\mathbf{I_R} = [I_1, \ldots, I_N]^T$ [11]

$$\mathbf{I_R} = \left(\mathbf{Z_R} + \mathbf{Z_L} \right)^{-1} \mathbf{V}_{oc}, \tag{5}$$

where $\mathbf{Z_L}$ is the equivalent multiport impedance matching load, $\mathbf{Z_R}$ is the impedance matrix of the receive antennas, with self-impedances and mutual impedances as the diagonal and off-diagonal elements, respectively.

The voltages across the loads $\mathbf{V_L} = [V_{L1}, \ldots, V_{LN}]^T$ are then

$$\mathbf{V_L} = \mathbf{Z_L}\mathbf{I_R} = \mathbf{Z_L}\left(\mathbf{Z_R} + \mathbf{Z_L} \right)^{-1}\mathbf{V}_{oc}, \tag{6}$$

From [10], the open-circuit voltage on the half-wavelength dipole antennas is given by

$$\mathbf{V}_{oc} = \mathbf{a}(\phi)E_0, \tag{7}$$

where E_0 is the electric field at the first antenna (at the origin of the coordinate system). Following the same approach as [10], we rewrite (6) as

$$\mathbf{V_L} = \underbrace{\frac{z_L}{z_A + z_L}\mathbf{Z_L}\left(\mathbf{Z_R} + \mathbf{Z_L} \right)^{-1}}_{C}\mathbf{a}(\phi)\underbrace{\frac{z_A + z_L}{z_L}}_{\tilde{g}}\underbrace{E_0}_{s_m(t)}, \tag{8}$$

where the constant $\pi\tilde{g}/\lambda$ is the response (or gain) of a single dipole element of impedance z_A with impedance matching load z_L located at the origin of the coordinate system, the electric field strength E_0 is equivalent to the signal $s_m(t)$, $\mathbf{C}$ is the coupling matrix for the multiport impedance matching, which is a generalization of single-port load matching [10], [12]. For our purpose, we assume that the single dipole is conjugate matched $z_L = z_A^*$, which is the optimum match for a single antenna.

Therefore, if we assume the noise from the receive circuits dominates, the signal model with coupling and matching becomes

$$\mathbf{y}(t) = \mathbf{C}\tilde{\mathbf{A}}\mathbf{s}(t) + \mathbf{n}(t), \tag{9}$$

where $\tilde{\mathbf{A}} = \tilde{g}\left[\mathbf{a}(\phi_1), \ldots, \mathbf{a}(\phi_M) \right]$. It should be noted that coupling compensation techniques on the signal processing level are unable to reverse the loss of antenna efficiency due to mismatch on the circuit level. Moreover, it can create other problems. For example, one approach to compensate for coupling is to pre-multiplying $\mathbf{y}(t)$ by $\mathbf{C}^{-1}$. However, if $\mathbf{C}^{-1}$ is ill-conditioned, this results in noise amplification.

III.   CRAMER-RAO BOUND

For the calculations of the conditional CRB [10], we further assume that (i) $N > M$, and the steering matrix $\tilde{\mathbf{A}}$ is full rank for distinct incident angles, (ii) the coupling matrix has full rank, i.e., $\mathbf{C}\tilde{\mathbf{A}}$ is also full rank. The CRB expression is then given by

$$CRB(\phi_1, \ldots, \phi_M) = \frac{\sigma^2}{2K}\left[\mathrm{Re}\left\{ \left(\mathbf{D}^H\mathbf{C}^H\mathbf{P}\mathbf{C}\mathbf{D} \right) \odot \mathbf{R_s}^T \right\} \right]^{-1}, \tag{10}$$

where
$$\mathbf{D} = \tilde{g}\left[\left. \frac{\partial \mathbf{a}(\phi)}{\partial \phi} \right|_{\phi = \phi_1}, \ldots, \left. \frac{\partial \mathbf{a}(\phi)}{\partial \phi} \right|_{\phi = \phi_M} \right],$$

$$\mathbf{P} = \mathbf{I}_N - \mathbf{C}\tilde{\mathbf{A}}\left(\tilde{\mathbf{A}}^H\mathbf{C}^H\mathbf{C}\tilde{\mathbf{A}} \right)^{-1}\tilde{\mathbf{A}}^H\mathbf{C}^H,$$

K is the number of samples for the received signals. The root mean squared error (RMSE) for the mth signal is given by the squared root of the mth diagonal element of the CRB matrix expression (10).
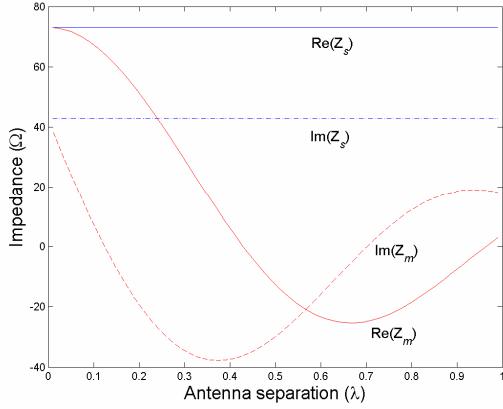
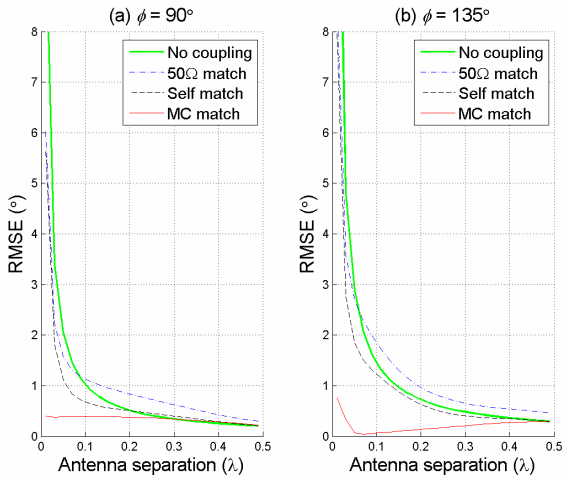Fig. 2   Self and mutual impedances of thin dipoles as a function of antenna separation in wavelength units.

Fig. 3   RMSE performance over different antenna separations and impedance matching conditions for DOA estimate of signal arriving at (a) $\phi = 90°$ and (b) $\phi = 135°$.

IV.   IMPEDANCE MATCHING NETWORKS

In this paper, we consider four matching conditions [7]-[9]: (i) no coupling and no impedance matching, with $\mathbf{C} = \mathbf{I}_N$. This is a popular assumption in array signal processing research, (ii) characteristic impedance (or 50Ω) match, with $\mathbf{Z}_L = Z_0\mathbf{I}$, (iii) self-impedance match $\mathbf{Z}_L = \text{diag}\left(\mathbf{Z}_R^*\right)$, where diag(.) retains only the diagonal elements of the matrix operand, and (iv) multiport conjugate (MC) match $\mathbf{Z}_L = \mathbf{Z}_R^*$ [11].

V.   NUMERICAL EXAMPLES

This section provides a numerical study of the impact of coupling and matching on the CRB performance of DOA estimation for closely coupled dipoles. We assume thin dipoles of thickness 0.02λ with the self impedance $Z_s = 73.1 + j43\,\Omega$ and mutual impedance $Z_m(d)$ that varies according to antenna separation d (see Fig. 2). The case of a 3-dipole ULA is investigated. In the following, the term "antenna separation d" denotes the separation distance between two adjacent antennas.

The signal-to-noise ratio (SNR) is assumed to be 10 dB and the number of samples $K = 200$.

A.   One Signal Scenario

We begin with a DOA scenario with only one signal arriving from the (a) $\phi = 90°$ (broadside), (b) $\phi = 135°$. The CRBs for the two single DOA cases are shown in Figs. 3(a) and 3(b), respectively. The y-axis limit is set at 8°, so that interesting features can be more clearly presented.

In Fig. 3, we observe that the RMSE results for the no coupling condition outperforms the coupling conditions of 50Ω match, self impedance and MC match for $d > 0.1\lambda, 0.2\lambda, 0.3\lambda$, respectively. However, all the curves approaches one another as the antenna separation increases to 0.5λ, confirming earlier studies which indicate that the coupling effect is small for conventional arrays where $d \approx 0.5\lambda$. The small offset observed between the 50Ω match and the other two coupled conditions at larger antenna separations is the result of a larger mismatch between the antenna self impedance and the 50Ω termination impedance, which leads to poorer efficiency. The problem of antenna mismatch or efficiency is further highlighted in Fig. 4, where the effective antenna patterns of the three dipoles at $d = 0.1\lambda$ for the four matching conditions are illustrated. The curves in Fig. 4 are normalized such that the omnidirectional pattern of the no coupling condition is at 0 dB. We note that the antenna gain is consistently less than 0 dB for the 50Ω match, even though the antenna patterns (of the three dipoles) are more diverse or dissimilar than the no coupling condition. As $d < 0.1\lambda$ in Fig. 3(a), the pattern diversity which exists for the 50Ω match enables it to outperform the no coupling condition, even at a reduced efficiency. For the self impedance match, even though the antenna patterns are similarly shaped as the 50Ω match (see Fig. 4(c)), it has better efficiency, which results in consistently superior performance to the 50Ω match. The advantage of using the MC match for closely coupled antennas is clearly observed in Fig. 3(a). As can be seen in Fig. 4(d), the antenna patterns of the three dipoles are significantly different from one another, and the gain of the middle antenna is significantly higher than 0 dB!

As the signal is moved from the broadside to $\phi = 135°$, i.e., Fig. 3(b), a similar trend as the broadside arrival may be observed. However, with the exception of the MC match, the performance of all other matching conditions is worse than the broadside arrival of Fig. 3(a). For the no coupling condition, it is well known that as the signal moves away from the broadside, the effective aperture of the ULA decreases, resulting in a poorer DOA estimate. Since the antenna patterns of the 50Ω and the self impedance match do not experience significant distortions, the aperture reduction effect dominates and consequently a poorer performance is obtained. On the other hand, since the antenna patterns of the MC match are significantly distorted, such that the pattern diversity can play a more dominant role, the CRB of this case outperforms the broadside arrival for $d \in (0.05\lambda, 0.4\lambda)$ (see Fig. 3(b)).
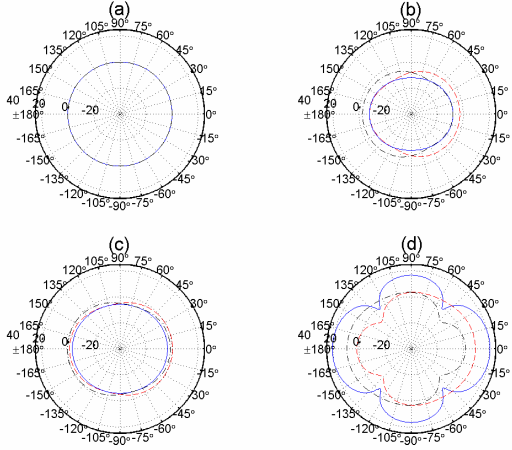
Fig. 4 Antenna patterns for different impedance matching conditions at $d = 0.1\lambda$: (a) No coupling, (b) 50Ω match, (c) Self match, and (d) MC match. The black dash-dotted line, blue solid line, and red dashed line indicate the antenna patterns for dipole 1, 2 and 3, respectively.
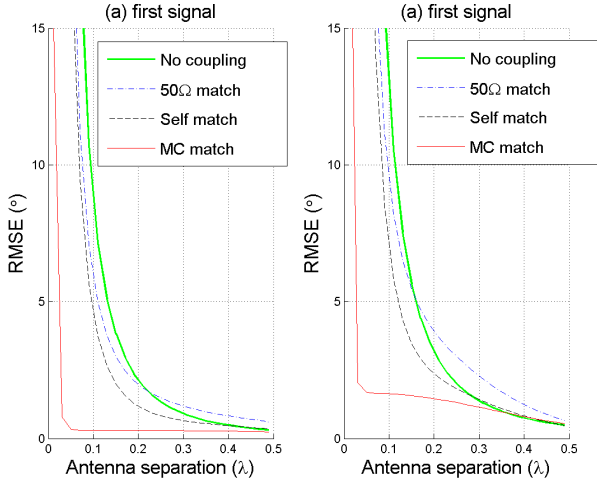

Fig. 5 RMSE performance of the first signal over different antenna separations and impedance matching conditions for DOA estimates of two signals arriving from (a) $\phi = 70°$, 110° and (b) $\phi = 115°$, 155°.

B. Two Signal Scenario

In the second scenario, two signals 40° apart arrive from (a) $\phi = 70°$, 110° and (b) $\phi = 115°$, 155°. The two signals of cases (a) and (b) are symmetrically located along the array broadside and 135°, respectively. The CRB performance for the first signal for cases (a) and (b) are shown in Figs. 5(a) and 5(b), respectively. The corresponding results for the second signal are given in Figs 6(a) and 6(b). The y-axis limit is set at 15°.

In general, Figs. 5 and 6 follow a similar trend as in Fig. 3. However, as expected of a more complicated signal scenario, the CRB performances for the two signal scenario is noticeably worse than the one signal scenario for small antenna separations.
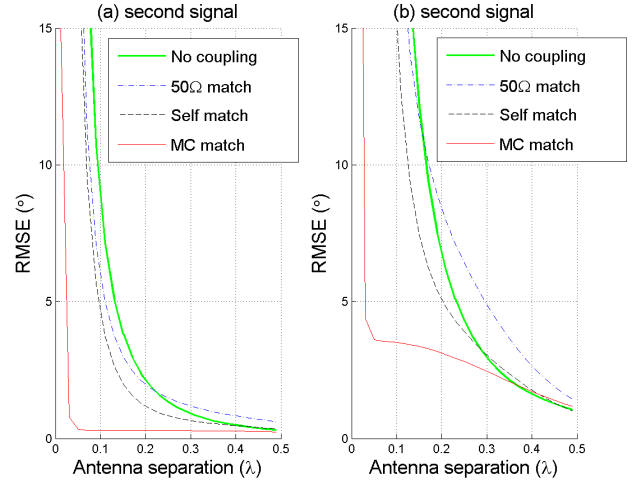

Fig. 6 RMSE performance of the second signal over different antenna separations and impedance matching conditions for DOA estimates of two signals arriving from (a) $\phi = 70°$, 110° and (b) $\phi = 115°$, 155°.

Another feature which differs significantly to the previous scenario is the behavior of the MC match, which rapidly deteriorates for $d < 0.05\lambda$. This could be in part due to the use of a dipole model with a thickness of comparable value to the antenna separation. Notwithstanding, the promising results as shown by MC match indicates another major benefit of implementing the multiport matching over the other matching conditions.

A comparison between the Fig. 5(a) and Fig. 6(a) with Fig. 5(b) and 6(b) reveals that an offset of the two signals (of 40° separation) from being symmetrical the array broadside result in poorer CRB performances for all matching conditions. Moreover, the worse performance among the two signals is demonstrated by the second signal, which is closer to the array endfire upon the offset. This is contrary to the single signal scenario, where an offset of the signal DOA can actually improve the DOA performance for the MC match.

VI. CONCLUSIONS

This paper presents a first study in the impact of matching on the DOA estimation performance of closely coupled arrays. We show that a proper matching impedance consideration can greatly improve the performance as compared to either the conventional characteristic (or 50Ω) impedance termination or the ideal no coupling condition favored by the array processing community. Therefore, the effect of impedance matching should be included in the study of array algorithms for closely coupled arrays, in order to achieve performance that is both realistic and optimum.

REFERENCES

[1] S. Andersson, B. Hagerman, H. Dam, U. Forssén, J. Karlsson, F. Kronestedt, S. Mazur, and K. J. Molnar, "Adaptive Antennas for GSM and TDMA Systems," IEEE Personal Commun., vol. 6., no. 3, pp. 74-86, Jun. 1999.

[2] http://www.arraycomm.com

[3]   J. Winters, "On the Capacity of Radio Communication Systems with Diversity in a Rayleigh Fading Environment," *IEEE J. Select. Areas Commun.*, vol. SAC-5, pp.871-878, Jun. 1987.

[4]   I. E. Telatar, "Capacity of multi-antenna Gaussian channels," *European Trans. Telecommun.*, vol. 10, pp. 585-595, 1999.

[5]   G. J. Foschini and M. J. Gans, "On limits of wireless communications in a fading environment when using multiple antennas," *Wireless Personal Communications (Kluwer Academic Publishers)*, vol. 6, pp. 311–335, Mar. 1998.

[6]   J. Avendal, Z. Ying, and B. K. Lau, "Multiband diversity antenna performance study for mobile phones," in *Proc. International Workshop on Antenna Technology* (iWAT), Cambridge, UK, Mar. 21-23, 2007.

[7]   J. W. Wallace and M. A. Jensen, "Termination-dependent diversity performance of coupled antennas: Network theory analysis," *IEEE Trans. Antennas Propagat.*, vol. 52, pp. 98-105, Jan. 2004.

[8]   J. W. Wallace and M. A. Jensen, "Mutual coupling in MIMO wireless systems: a rigorous network theory analysis," *IEEE Trans. Wireless Commun.*, vol. 3, pp. 1317-1325, Jul. 2004.

[9]   B. K. Lau, J. B. Andersen, G. Kristensson, and A. F. Molisch, "Impact of matching network on bandwidth of compact antenna arrays," *IEEE Trans. Antennas Propagat.*, vol. 54, no. 11, pp. 3225-3238, Nov. 2006.

[10]   T. Svantesson, "Direction finding in the presence of mutual coupling," Licentiate Thesis (Technical report no. 307L), Department of Signals and Systems, Chalmers University of Technology, Sweden, 1999.

[11]   R. Vaughan and J. B. Andersen, *Channels, Propagation and Antennas for Mobile Communications*, The IEE, 2003.

[12]   J. B. Andersen and B. K. Lau, "On closely coupled dipoles in a random field," *IEEE Antennas and Wireless Propagat. Lett.*, vol. 5, no. 1, pp. 73-75, 2006.